Electronic Supplementary Material (ESI) for Inorganic Chemistry Frontiers.

Supporting Information

Modulating the peripheral large steric hindrance of iridium complex for achieving narrowband emission and pure red OLED with EQE up to 32.0%

Changjin Ou,[‡a] Yu-Chen Qiu,[‡a] Chenhui Cao,[c] Hui Zhang,[a] Juan Qin,*[a] Zhen-Long Tu,*[b] Jian Shi[a] and Zheng-Guang Wu*[a]

[a.] *School of Chemistry and Chemical Engineering, Nantong University, Nantong, Jiangsu, 226019, P. R. China. E-mail: qinjuan880816@ntu.edu.cn, wuzhengguang_zy@163.com*

[b.] *Research Centre for Information Technology, Shenzhen Institute of Information Technology, Shenzhen, 518172 P. R. China. E-mail: tuzhenlong@qq.com*

[c.] *Anhui Sholon New Material Technology Co., Ltd., Chuzhou, Anhui, 239500, P. R. China.*

[‡]*Changjin Ou and Yu-Chen Qiu contributed equally to this work.*

E-mail: wuzhengguang_zy@163.com

1. General Descriptions

1.1 Materials and measurements

All reagents and chemicals were purchased from commercial sources and used without further purification. ^{1}H NMR, ^{19}F NMR, ^{13}C NMR spectra were measured on a Bruker AM 400 spectrometer. High resolution mass spectra (HRMS) were measured with a LTQ-Orbitrap XL (Thermofisher, U. S. A.). Absorption and photoluminescence spectra were measured on a UV-3100 spectrophotometer and a Hitachi F-4600 photoluminescence spectrophotometer, respectively. The decay lifetimes were measured with an Edinburgh Instruments FLS-920 fluorescence spectrometer. The absolute photoluminescence quantum yields (Φ) was measured with HORIBA FL-3 fluorescence spectrometer. Cyclic voltammetry measurements were conducted on a MPI-A multifunctional electrochemical and chemiluminescent system (Xi'an Remex Analytical Instrument Ltd. Co., China) at room temperature, with a polished Pt plate as the working electrode, platinum thread as the counter electrode and Ag-$AgNO_3$ (0.1 M) in CH_3CN as the reference electrode, *tetra*-n-butylammonium perchlorate (0.1 M) was used as the supporting electrolyte, using Fc^+/Fc as the internal standard, the scan rate was 0.1 V/s.

1.2 Theoretical calculation.

The density functional theory (DFT) and time-dependent DFT (TD-DFT) calculations were carried out with Gaussian 09 software package. The geometries of the ground state (S0) were fully optimized with the B3LYP exchange-correlation functional using the LANL2DZ basis set for iridium atom and the 6-31G** basis set for the other atoms both in vacuum and in CH_2Cl_2 (C-PCM27 solvent model). Vibrational frequency calculations were performed to validate that they are minima on potential energy surface. On the basis of the optimized S0 molecular structures in solvent, TD-DFT calculation was performed. Solvent effect was also considered by using C-PCM model. Frontier molecular orbitals were visualized using Gauss View, and their quantified compositions in percentage on different parts were given by QMForge.

1.3 Fabrication and measurements of OLEDs

Indium-tin-oxide (ITO) coated glass with a sheet resistance of 10 Ω/sq was used as the anode substrate. Prior to film deposition, patterned ITO substrates were cleaned with detergent, rinsed in

de-ionized water, dried in an oven, and finally treated with oxygen plasma for 5 minutes at a pressure of 10 Pa to enhance the surface work function of ITO anode (from 4.7 to 5.1 eV). All the organic layers were deposited with the rate of 0.1 nm/s under high vacuum ($\leq 2\times10^{-5}$ Pa). The doped layers were prepared by co-evaporating dopant and host material from two individual sources, and the doping concentrations were modulated by controlling the evaporation rate of dopant. LiF and Al were deposited in another vacuum chamber ($\leq 8.0\times10^{-5}$ Pa) with the rates of 0.01 and 1 nm s^{-1}, respectively, without being exposed to the atmosphere. The thicknesses of these deposited layers and the evaporation rate of individual materials were monitored in vacuum with quartz crystal monitors. A shadow mask was used to define the cathode and to make ten emitting dots with the active area of 9 mm^2 (3 mm×3 mm) on each substrate. Device performances were measured by using a programmable Keithley source measurement unit (Keithley 2400 and Keithley 2000) with a silicon photodiode. The EL spectra were measured with a calibrated Hitachi F−7000 fluorescence spectrophotometer. Based on the uncorrected EL fluorescence spectra, the Commission Internationale de l'Eclairage (CIE) coordinates were calculated using the test program of Spectrascan PR650 spectrophotometer. The EQE of EL devices were calculated based on the photo energy measured by the photodiode, the EL spectrum, and the current pass through the device.

2. Experimental Section

2.1 Synthesis routes and procedures for the iridium complexes

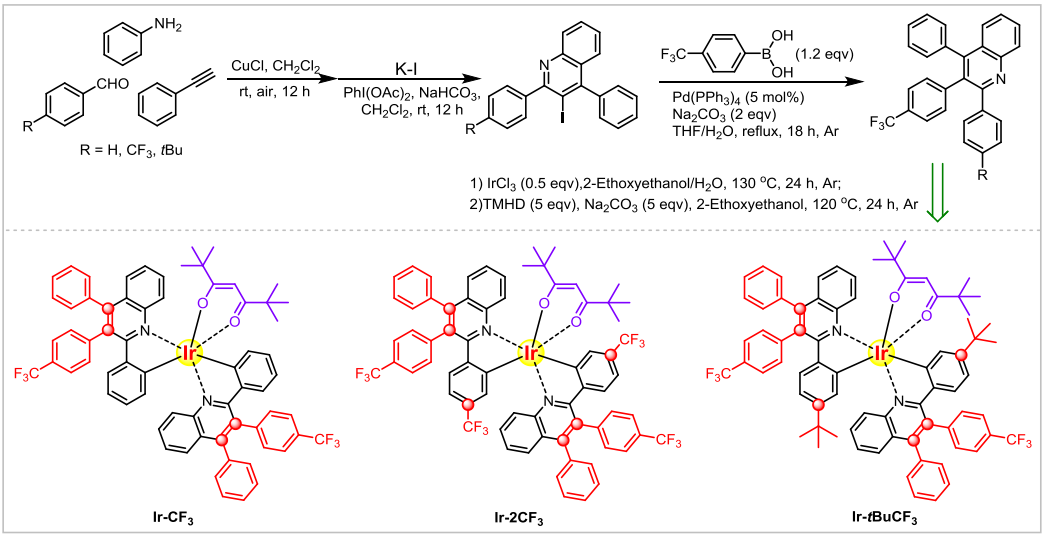

2.1.1 Synthesis of 3-iodoquinolines

To a solution of aromatic amine (5 mmol, 0.46 g), benzaldehyde (5 mmol, 0.53 g), alkyne (5 mmol, 0.51 g) and CuCl (0.5 mmol, 49 mg) in CH_2Cl_2 (30 mL), the mixture was stirred at room temperature. After 12 h, halide salt KI (7.5 mmol, 1.25 g) was added and then $PhI(OAc)_2$ (10 mmol, 3.22 g) is slowly added in three batches and the reaction mixture was stirred for another 12 h at room temperature under air. The crude mixture was purified by flash column chromatography to afford the intermediate 3-iodoquinolines (R=H, CF_3, *t*Bu) with the yields of 72% (1.47 g), 70% (1.66 g) and 75% (1.74 g), respectively.

2.1.2 General procedure for the preparation of main ligands

For **L1**, under argon, to a solution of intermediate 3-iodoquinoline (2.0 mmol, 0.81 g), 4-(trifluoromethyl)phenylboronic acid (2.4 mmol, 0.46 g), $Pd(PPh_3)_4$ (5 mol%, 0.12 g) and Na_2CO_3 (4.0 mmol, 0.42 g) in THF(60 mL)/H_2O (20 mL), the mixture was stirred at reflux for 18 h. After the reaction was cooled to room temperature, H_2O (100 mL) and CH_2Cl_2 (40 mL) was added. Then the organic phase was concentrated and purified by flash chromatography on silica gel to give the desired main ligand **L1** with the yield of 75% (0.64g). Using this method, **L2** and **L3** can also be smoothly synthesized with the yields of 78% (0.77 g) and 70% (0.67 g), respectively.

2.1.3 General procedure for the preparation of Ir(III) complexes

A mixture of main ligand **L1** (0.25 mmol, 0.11g) and $IrCl_3$ (0.1 mmol, 29 mg) in 2-ethoxyethanol and water (16 mL, 3 : 1, v/v) was stirred at 130 ℃ for 24 h under argon. After cooling, the solid precipitate was filtered to obtain crude cyclometalated Ir(III) chloro-bridged dimer. Then, the slurry of crude chloro-bridged dimer, Na_2CO_3 (1 mmol, 0.11g) and TMHD (1 mmol, 0.18 g) in 2-ethoxyethanol (20 mL) were reacted at 120 ℃ for 24 h. The solvent was evaporated at low pressure, and the mixture was poured into water. Next, the mixture was extracted with CH_2Cl_2 and then chromatographed to give the iridium complex **Ir-CF_3** with 52% yield (64 mg). Using this method, **Ir-2CF_3** and **Ir-*t*BuCF_3** can also be smoothly synthesized with the yields of 50% (68 mg) and 41% (55 mg), respectively.

2.2 Characterization data

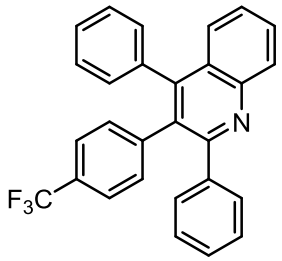

L1

2,4-diphenyl-3-(4-(trifluoromethyl)phenyl)quinoline

^{1}H NMR (400 MHz, $CDCl_3$) δ 8.27 (d, J = 8.3 Hz, 1H), 7.76 (ddd, J = 8.3, 6.8, 1.4 Hz, 1H), 7.63 – 7.55 (m, 1H), 7.48 (ddd, J = 8.2, 6.8, 1.1 Hz, 1H), 7.37 – 7.19 (m, 10H), 7.11 (dd, J = 6.6, 3.0 Hz, 2H), 7.02 (d, J = 8.0 Hz, 2H).

^{13}C NMR (101 MHz, $CDCl_3$) δ 158.54 (s), 147.94 (s), 147.57 (s), 142.42 (s), 140.68 (s), 136.40 (s), 131.62 (d, J = 16.9 Hz), 130.20 (s), 129.98 – 129.69 (m), 128.93 (s), 128.61 (s), 128.29 (s), 127.99 (d, J = 13.8 Hz), 127.69 (s), 126.78 (d, J = 18.8 Hz), 126.49 (s), 125.40 (s), 124.31 (q, J = 3.8 Hz), 122.69 (s).

^{19}F NMR (376 MHz, $CDCl_3$) δ -62.51.

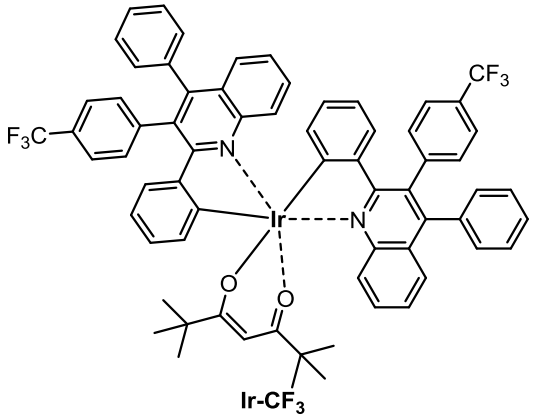

Ir-CF_3

^{1}H NMR (400 MHz, $CDCl_3$) δ 8.41 (dd, J = 7.0, 2.8 Hz, 2H), 7.72 (d, J = 8.0 Hz, 2H), 7.63 (d, J = 8.4 Hz, 2H), 7.52 – 7.45 (m, 6H), 7.43 – 7.40 (m, 2H), 7.36 – 7.32 (m, 6H), 7.28 (d, J = 7.4 Hz, 2H), 7.16 (t, J = 7.5 Hz, 2H), 6.72 (dd, J = 6.2, 1.9 Hz, 2H), 6.66 (d, J = 7.6 Hz, 2H), 6.50 – 6.44 (m, 6H), 4.90 (s, 1H), 0.85 (s, 18H).

^{13}C NMR (101 MHz, $CDCl_3$) δ 193.87 (s), 168.65 (s), 153.83 (s), 149.36 (s), 148.28 (s), 147.62 (s), 142.74 (s), 137.29 (s), 136.28 (s), 131.75 (s), 131.47 (s), 130.50 (d, *J* = 13.2 Hz), 129.94 (s), 129.38 (t, *J* = 16.3 Hz), 128.44 (s), 127.96 – 127.44 (m), 126.24 (d, *J* = 14.2 Hz), 125.58 (s), 125.38 (s), 125.05 (s), 119.78 (s), 88.23 (s), 40.96 (s), 28.19 (s).

^{19}F NMR (376 MHz, $CDCl_3$) δ -62.47.

HRMS (ESI) *m/z* calcd for $C_{67}H_{53}F_6IrN_2O_2H$ [M+H]: 1225.3719, found: 1225.3719.

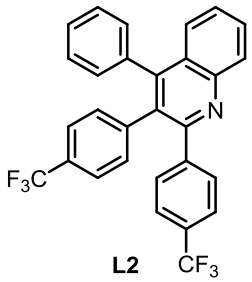

L2

4-phenyl-2,3-bis(4-(trifluoromethyl)phenyl)quinoline

^{1}H NMR (400 MHz, $CDCl_3$) δ 8.26 (d, *J* = 8.4 Hz, 1H), 7.79 (ddd, *J* = 8.3, 6.9, 1.3 Hz, 1H), 7.62 (d, *J* = 8.2 Hz, 1H), 7.54 – 7.44 (m, 5H), 7.31 (dd, *J* = 7.1, 4.0 Hz, 5H), 7.12 (dt, *J* = 4.1, 3.4 Hz, 2H), 7.03 (d, *J* = 8.1 Hz, 2H).

^{13}C NMR (101 MHz, $CDCl_3$) δ 156.87 (s), 148.42 (s), 147.55 (s), 144.26 (s), 141.85 (s), 136.06 (s), 131.64 (s), 131.29 (s), 130.39 – 129.99 (m), 129.80 (s), 129.03 (s), 128.71 (s), 128.14 (s), 127.88 (s), 127.38 (s), 126.71 (d, *J* = 11.4 Hz), 125.40 (s), 125.27 (s), 124.95 – 124.35 (m), 122.63 (d, *J* = 12.6 Hz).

^{19}F NMR (376 MHz, $CDCl_3$) δ -62.57, -62.64.

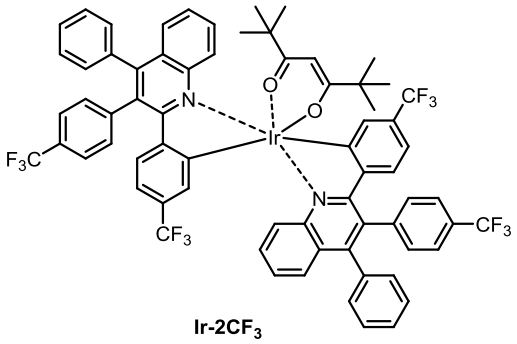

Ir-2CF_3

^{1}H NMR (400 MHz, $CDCl_3$) δ 8.25 – 8.12 (m, 2H), 7.60 (q, *J* = 8.4 Hz, 4H), 7.53 (d, *J* = 7.7 Hz, 2H), 7.49 – 7.46 (m, 2H), 7.43 – 7.36 (m, 6H), 7.33 – 7.27 (m, 4H), 7.23 (t, *J* = 7.5 Hz, 2H), 7.10 (t, *J* = 7.5 Hz, 2H), 6.83 (s, 2H), 6.66 (dd, *J* = 8.6, 1.4 Hz, 2H), 6.59 (d, *J* = 7.6 Hz, 2H), 6.46 (d, *J* = 8.5 Hz, 2H), 4.82 (s, 1H), 0.76 (s, 18H).

^{13}C NMR (101 MHz, $CDCl_3$) δ 194.02 (s), 167.25 (s), 152.31 (s), 151.38 (s), 150.22 (s), 148.12 (s), 142.20 (s), 135.90 (s), 133.16 (s), 131.83 (s), 131.31 (s), 131.04 (s), 130.65 (d, J = 12.8 Hz), 130.22 – 129.83 (m), 129.40 (d, J = 12.8 Hz), 128.47 (s), 127.85 (d, J = 12.8 Hz), 127.41 (s), 126.97 (s), 126.59 (s), 125.53 (d, J = 12.8 Hz), 117.09 (s), 88.50 (s), 41.01 (s), 28.20 (s).

HRMS (ESI) *m/z* calcd for $C_{67}H_{53}F_6IrN_2O_2H$ [M+H]: 1361.3466, found: 1361.3466.

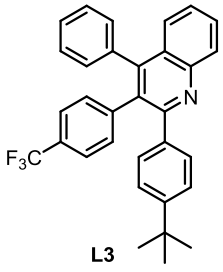

L3

^{1}H NMR (400 MHz, $CDCl_3$) δ 8.26 (d, *J* = 8.4 Hz, 1H), 7.79 – 7.70 (m, 1H), 7.58 (d, *J* = 7.9 Hz, 1H), 7.47 (dd, *J* = 11.1, 4.0 Hz, 1H), 7.31 – 7.21 (m, 9H), 7.11 (dd, *J* = 6.5, 2.9 Hz, 2H), 7.03 (d, *J* = 8.0 Hz, 2H), 1.26 (s, 9H).

^{13}C NMR (101 MHz, $CDCl_3$) δ 158.53 (s), 150.96 (s), 147.82 (s), 147.58 (s), 142.56 (s), 137.70 (s), 136.49 (s), 131.63 (d, *J* = 18.8 Hz), 130.21 (s), 129.75 (s), 129.54 (s), 128.52 (s), 128.11 (d, *J* = 17.3 Hz), 127.63 (s), 126.68 (d, *J* = 4.6 Hz), 126.40 (s), 124.89 (s), 124.26 (d, *J* = 3.8 Hz), 34.55 (s), 31.23 (s).

^{19}F NMR (376 MHz, $CDCl_3$) δ -62.50.

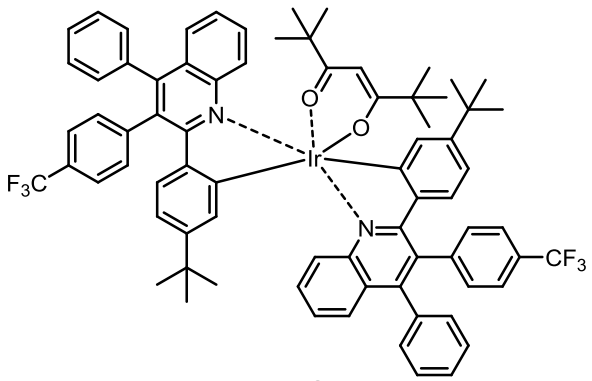

Ir-*t*BuCF$_3$

^{1}H NMR (400 MHz, $CDCl_3$) δ 8.31 (d, *J* = 7.4 Hz, 2H), 7.74 – 7.63 (m, 4H), 7.51 (s, 6H), 7.38 (dd, *J* = 23.0, 6.9 Hz, 8H), 7.18 (d, *J* = 7.1 Hz, 4H), 6.77 – 6.65 (m, 4H), 6.50 (d, *J* = 8.3 Hz, 2H), 6.36 (d, *J* = 8.4 Hz, 2H), 4.91 (s, 1H), 0.87 (s, 36H).

^{13}C NMR (101 MHz, $CDCl_3$) δ 192.73 (s), 166.99 (s), 153.75 (s), 148.50 (s), 147.97 (s), 147.17 (s), 144.19 (s), 141.88 (s), 135.48 (s), 133.46 (s), 130.84 (s), 130.37 (s), 129.55 (s), 129.31 (s), 128.87 (s), 128.30 (d, *J* = 10.8 Hz), 128.00 (s), 127.22 (s), 126.99 (s), 126.49 (s), 125.10 (s), 124.55 (d, *J* = 10.8 Hz), 116.18 (s), 87.10 (s), 39.86 (s), 32.93 (s), 29.88 (s), 27.22 (s).

^{19}F NMR (376 MHz, $CDCl_3$) δ -62.37.

HRMS (ESI) *m/z* calcd for $C_{67}H_{53}F_6IrN_2O_2H$ [M+H]: 1337.4971, found: 1337.4970.

2.3 NMR Spectra

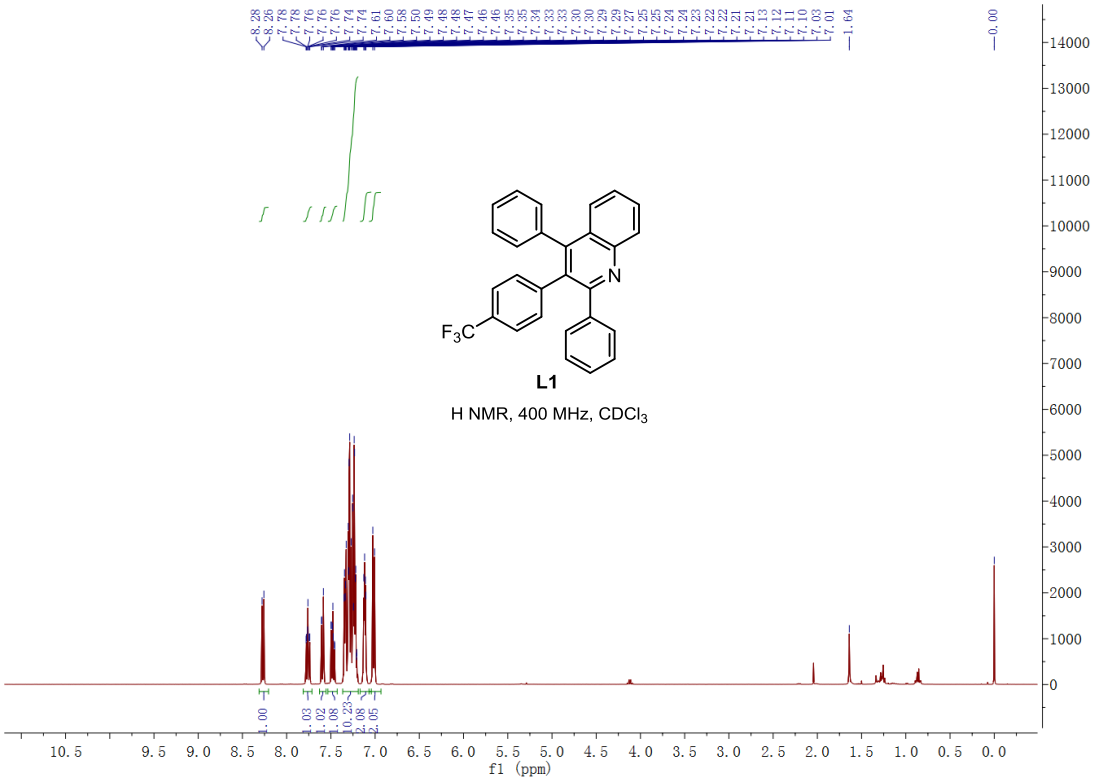

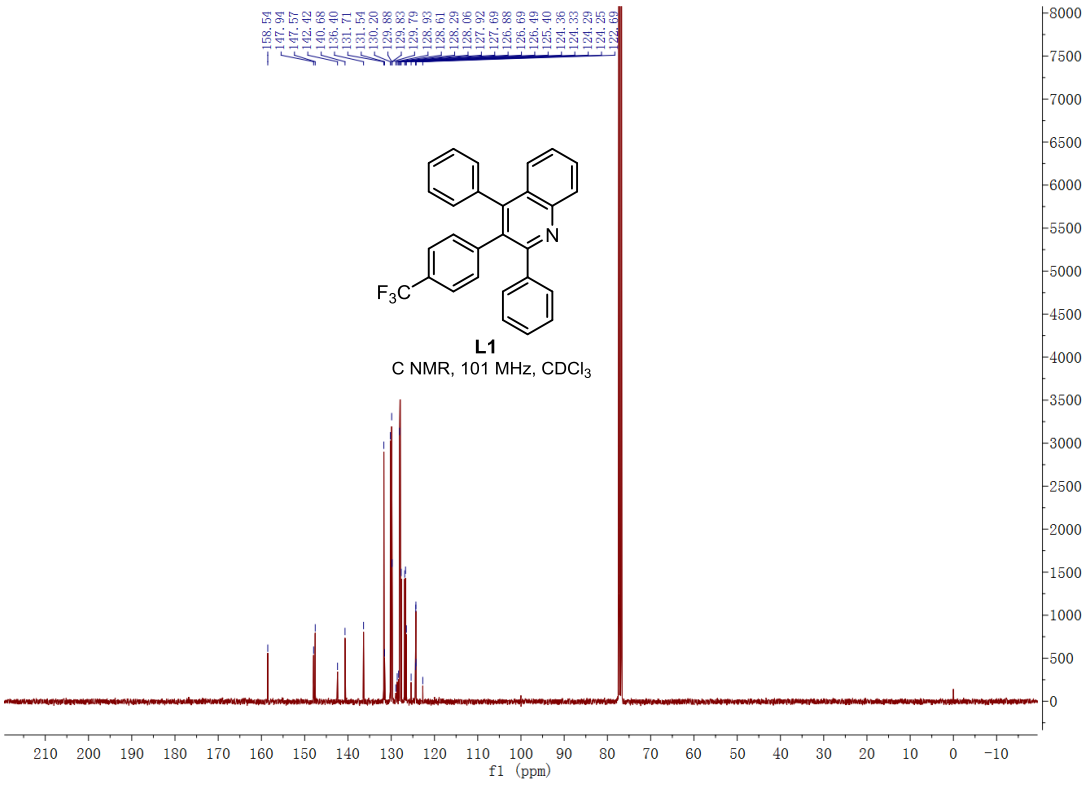

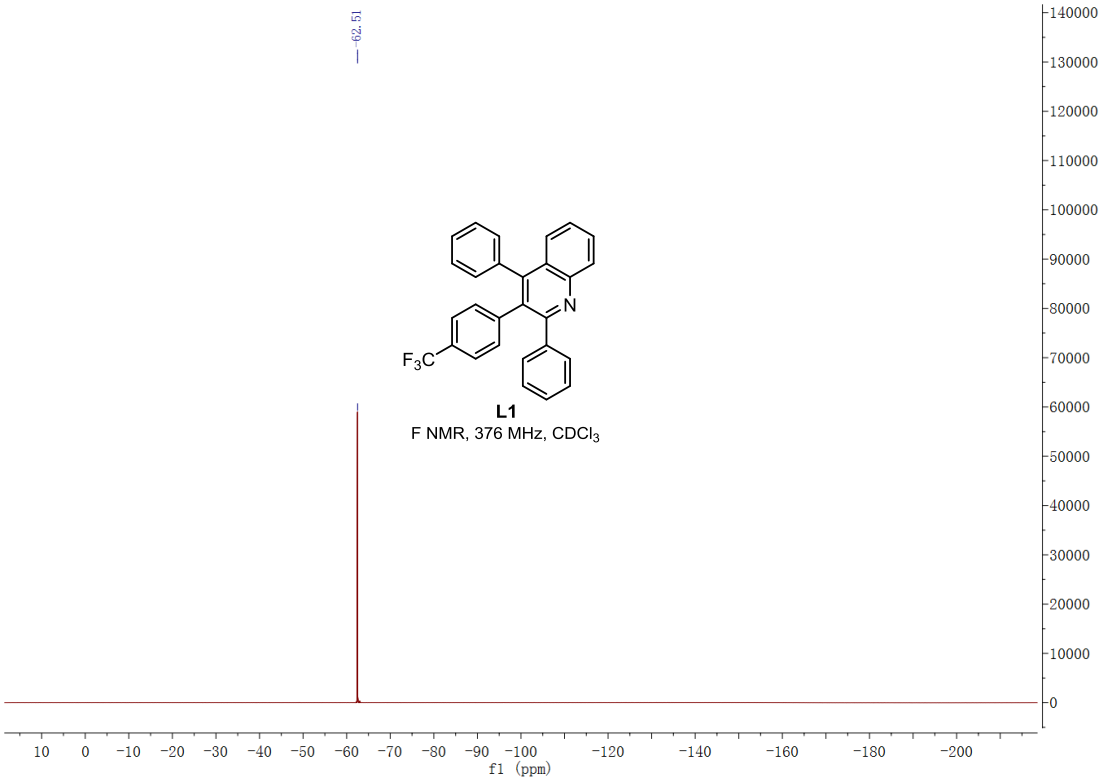

L1

F NMR, 376 MHz, $CDCl_3$

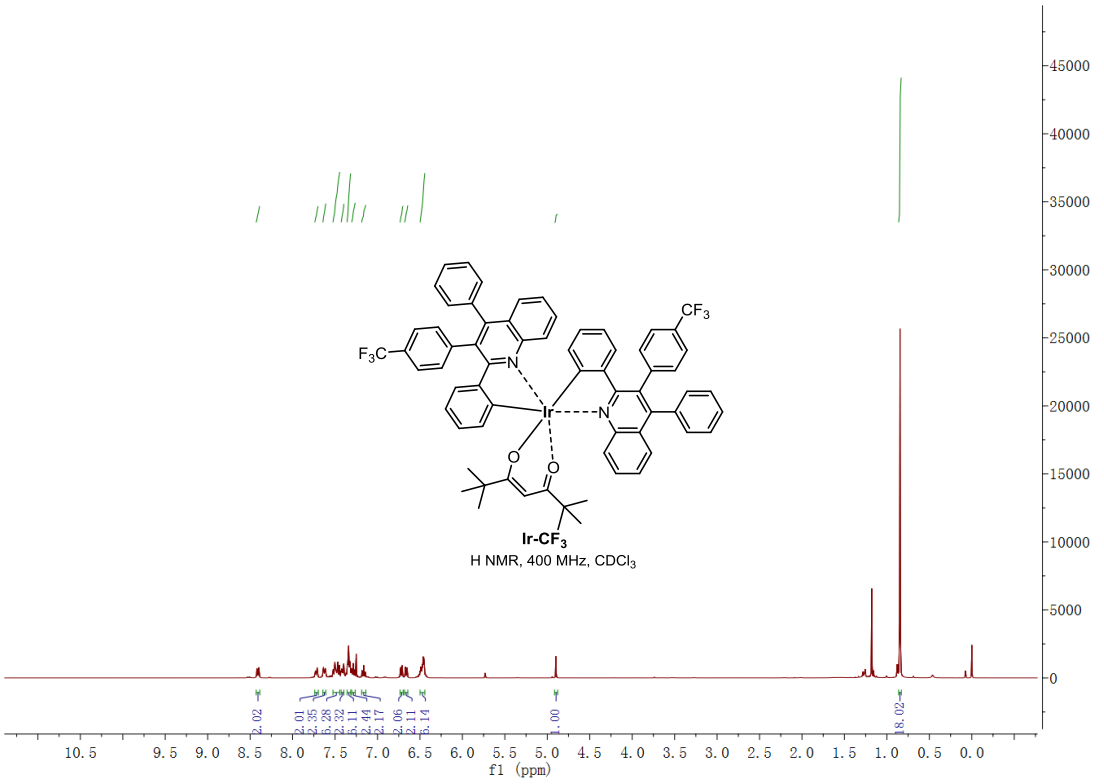

Ir-CF_3

H NMR, 400 MHz, $CDCl_3$

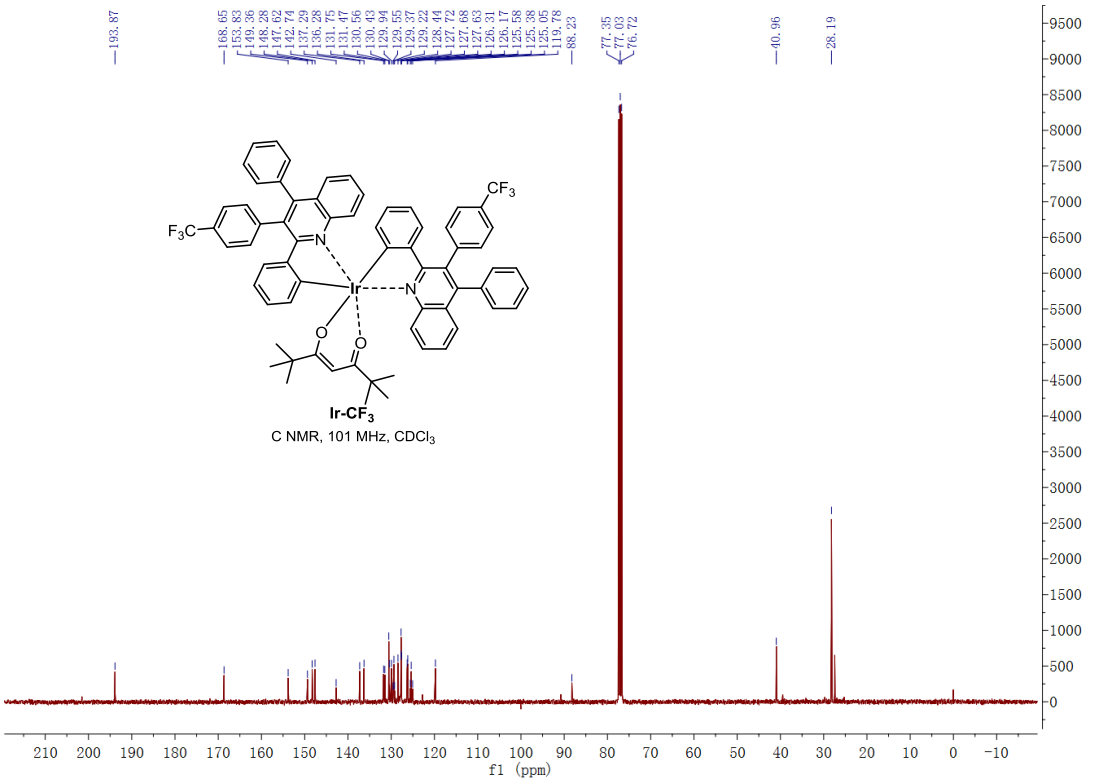
193.87
168.65
153.83
149.36
148.28
147.62
142.74
137.29
136.28
131.75
131.47
130.56
130.43
129.94
129.55
129.37
129.22
128.44
127.72
127.68
127.63
126.31
126.17
125.58
125.38
125.05
119.78
88.23
77.35
77.03
76.72
40.96
28.19
CF3
F3C
N
Ir
N
O
O
Ir-CF3
C NMR, 101 MHz, CDCl3
f1 (ppm)

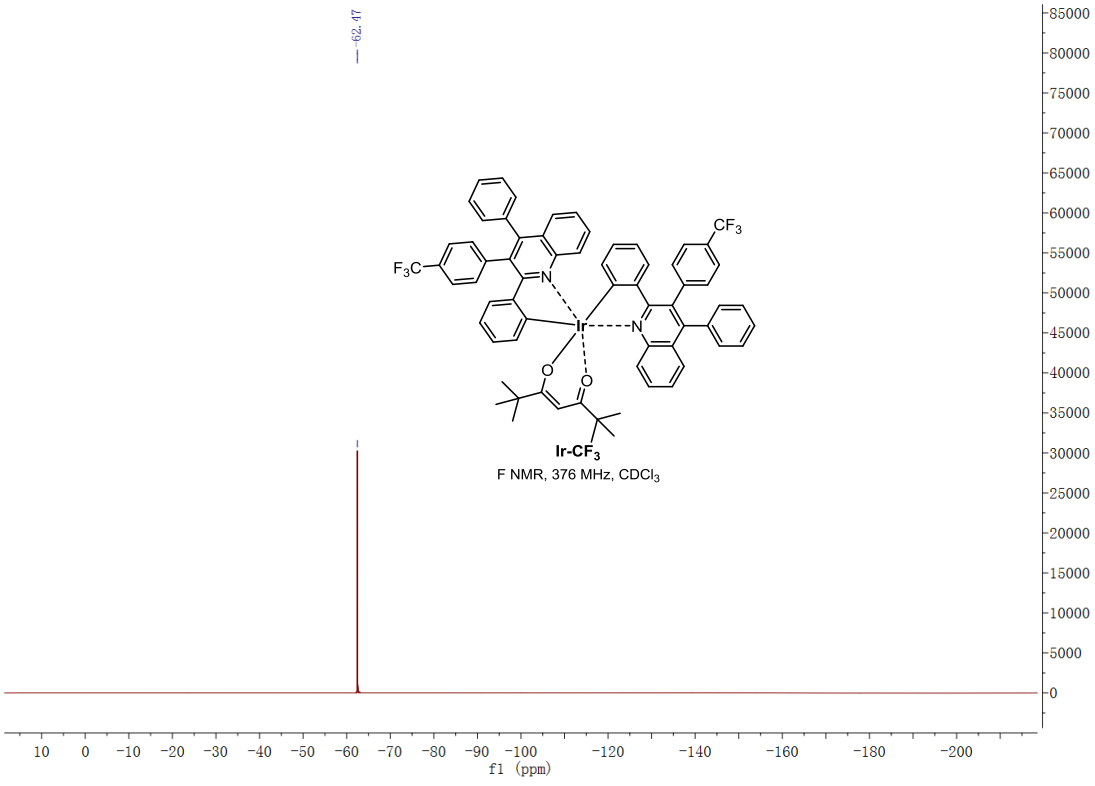
62.47
CF3
F3C
N
Ir
N
O
O
Ir-CF3
F NMR, 376 MHz, CDCl3
f1 (ppm)

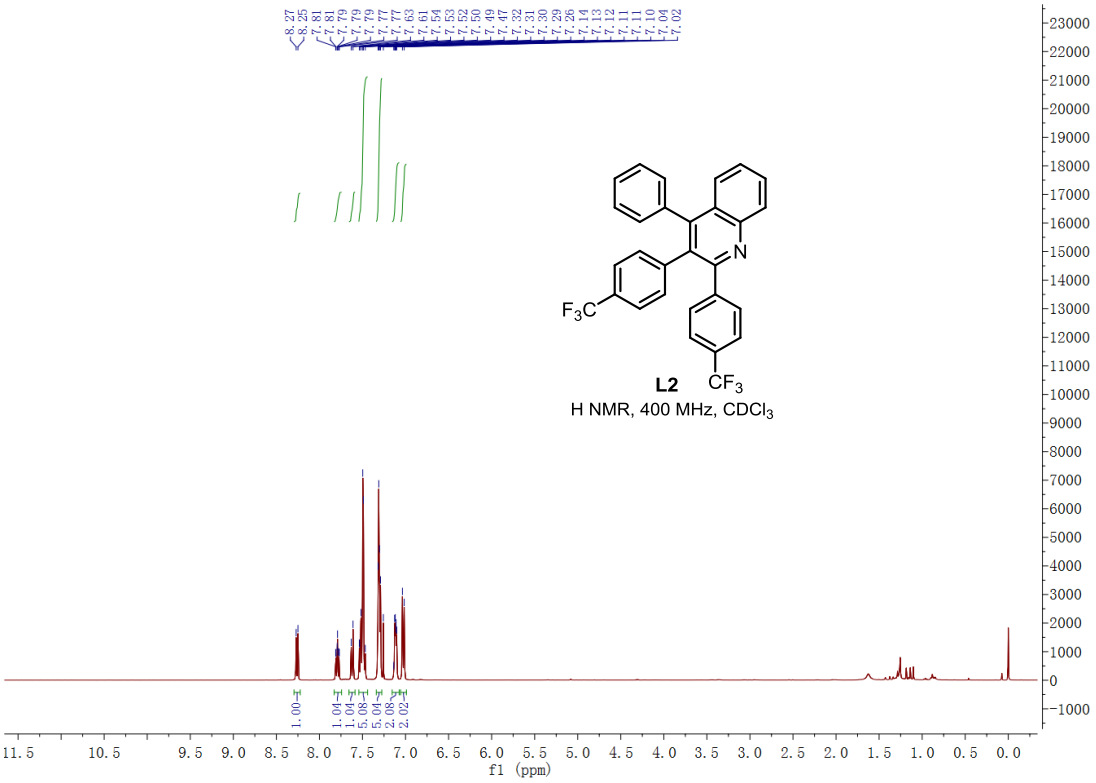

L2

H NMR, 400 MHz, $CDCl_3$

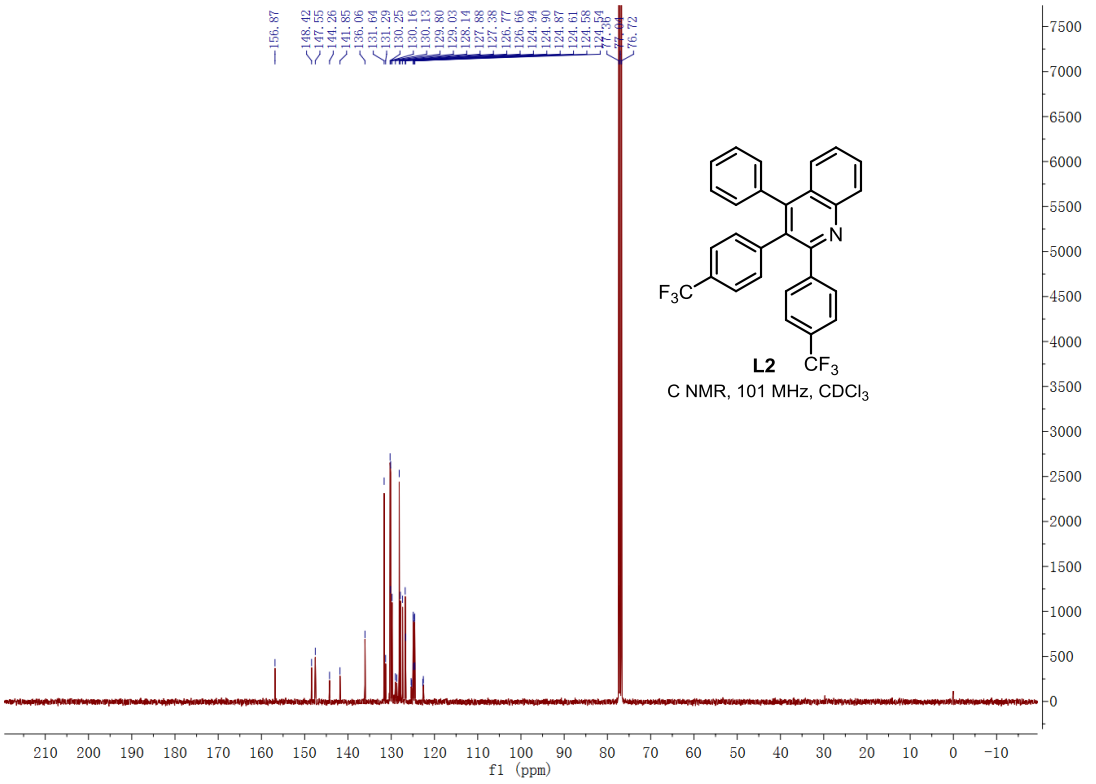

L2

C NMR, 101 MHz, $CDCl_3$

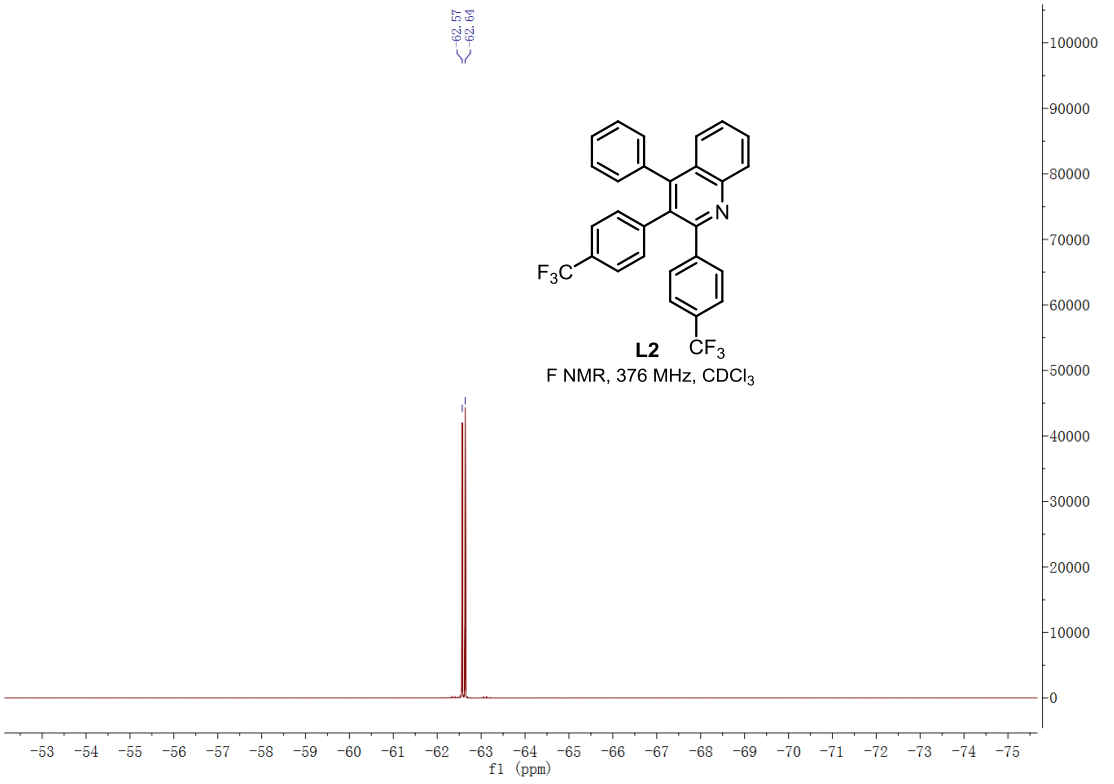
-62.57
-62.64
F3C
N
CF3
L2
F NMR, 376 MHz, CDCl3
f1 (ppm)

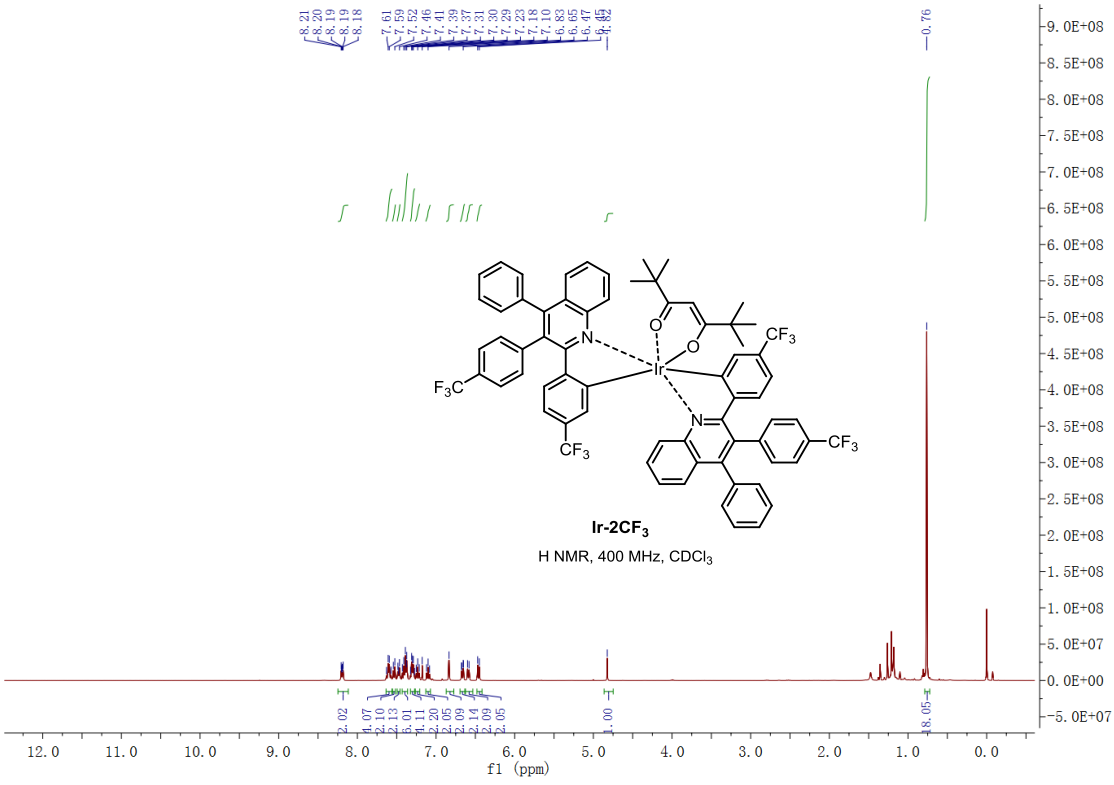
8.21
8.20
8.19
8.19
8.18
7.61
7.59
7.52
7.46
7.41
7.39
7.37
7.31
7.30
7.29
7.23
7.18
7.10
6.83
6.65
6.47
6.45
6.42
0.76
F3C
N
Ir
O
O
CF3
CF3
CF3
Ir-2CF3
H NMR, 400 MHz, CDCl3
2.02
1.07
2.19
2.01
1.11
2.20
2.05
2.09
2.14
2.09
2.05
1.00
8.05
f1 (ppm)

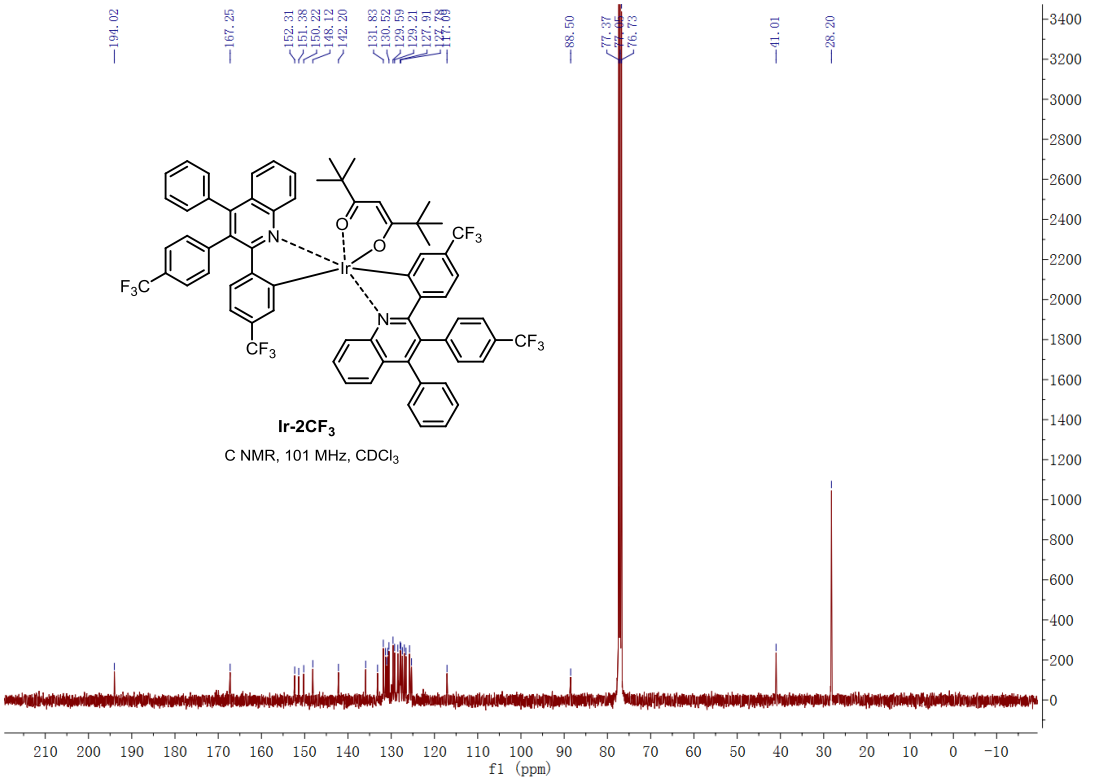

Ir-2CF$_3$

C NMR, 101 MHz, $CDCl_3$

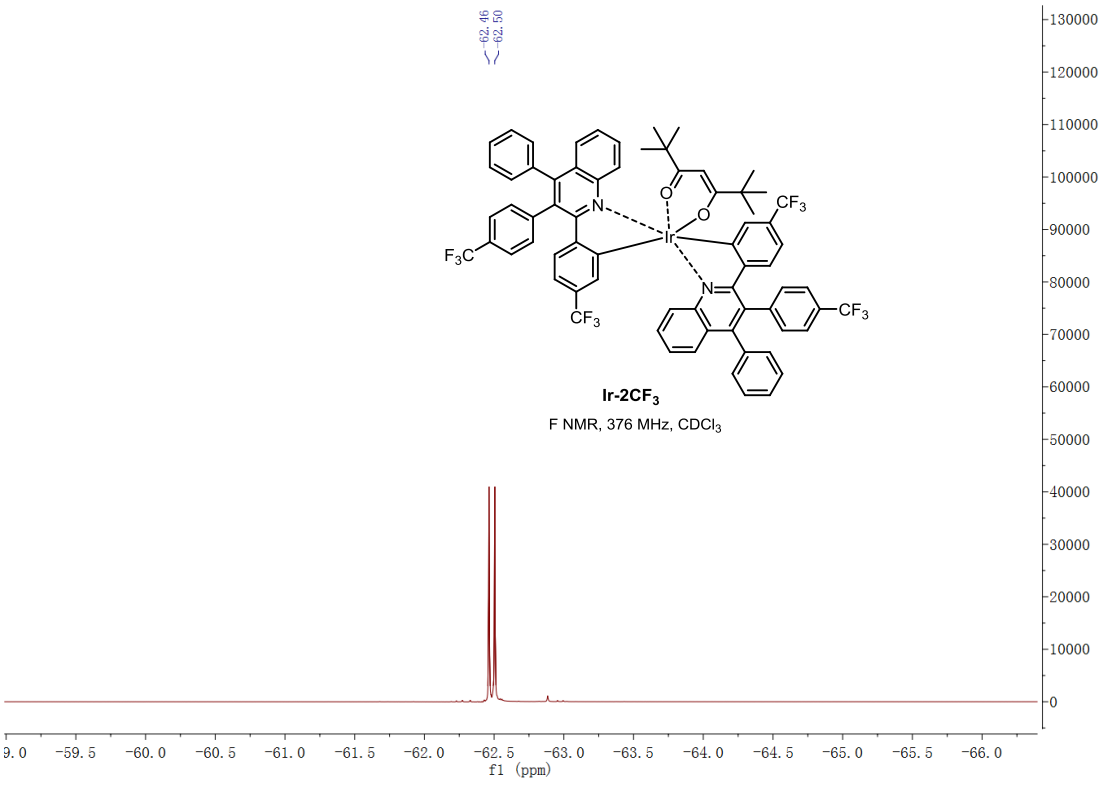

Ir-2CF$_3$

F NMR, 376 MHz, $CDCl_3$

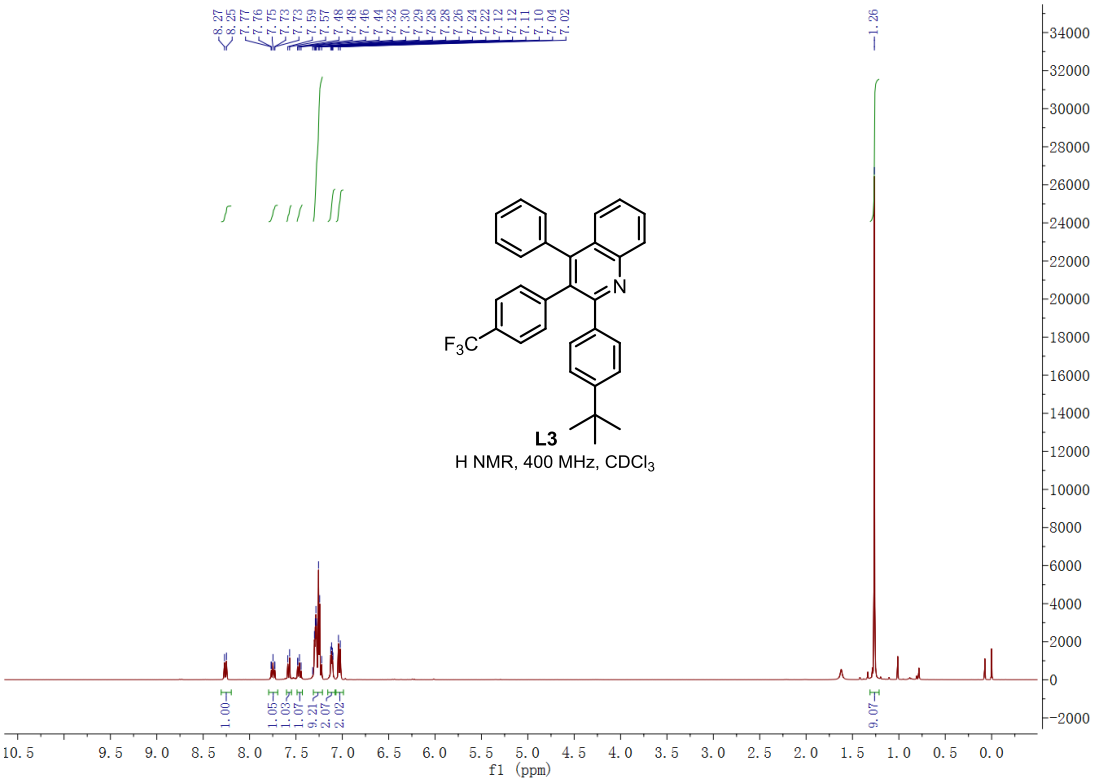
8.27
8.25
7.77
7.76
7.75
7.73
7.73
7.59
7.57
7.48
7.48
7.46
7.44
7.32
7.30
7.29
7.28
7.28
7.26
7.24
7.22
7.12
7.12
7.11
7.10
7.04
7.02
1.26
F3C
N
L3
H NMR, 400 MHz, CDCl3
1.00
1.05
1.03
1.07
9.21
2.07
2.02
9.07
f1 (ppm)

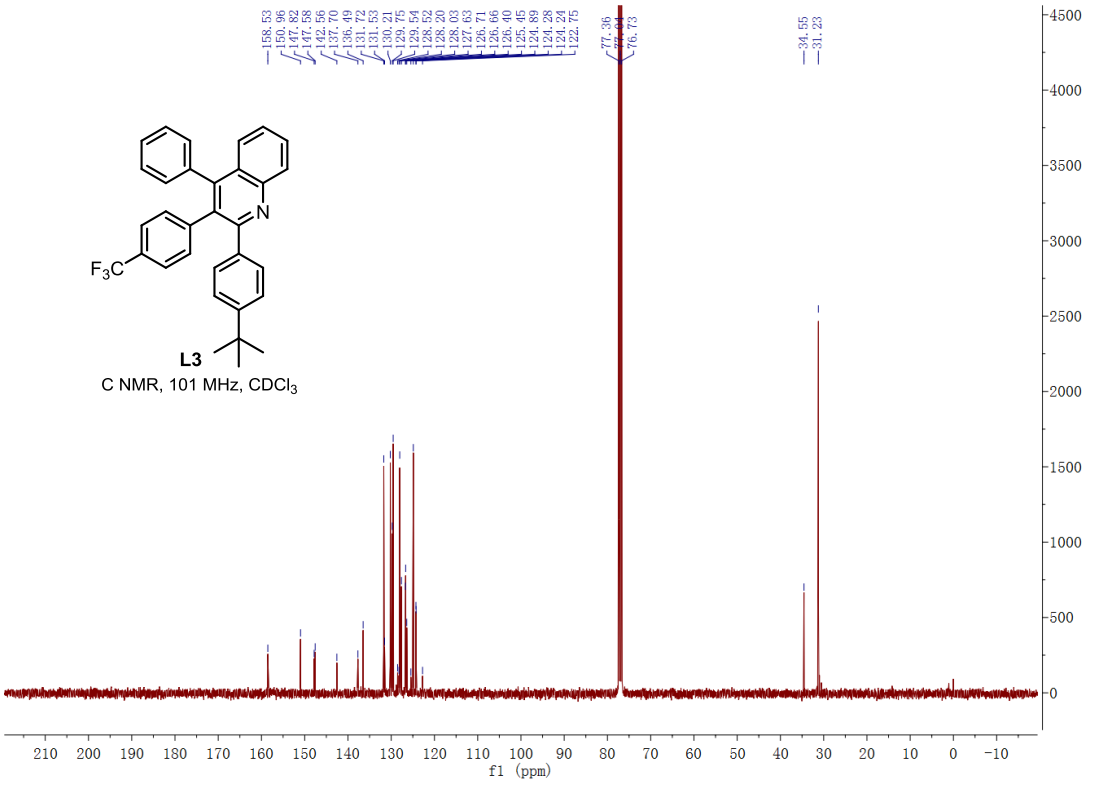
158.53
150.96
147.82
147.58
142.56
137.70
136.49
131.72
131.53
130.21
129.75
129.54
128.52
128.20
128.03
127.63
126.71
126.66
126.40
125.45
121.89
121.28
121.24
122.75
77.36
77.04
76.73
34.55
31.23
F3C
N
L3
C NMR, 101 MHz, CDCl3
f1 (ppm)

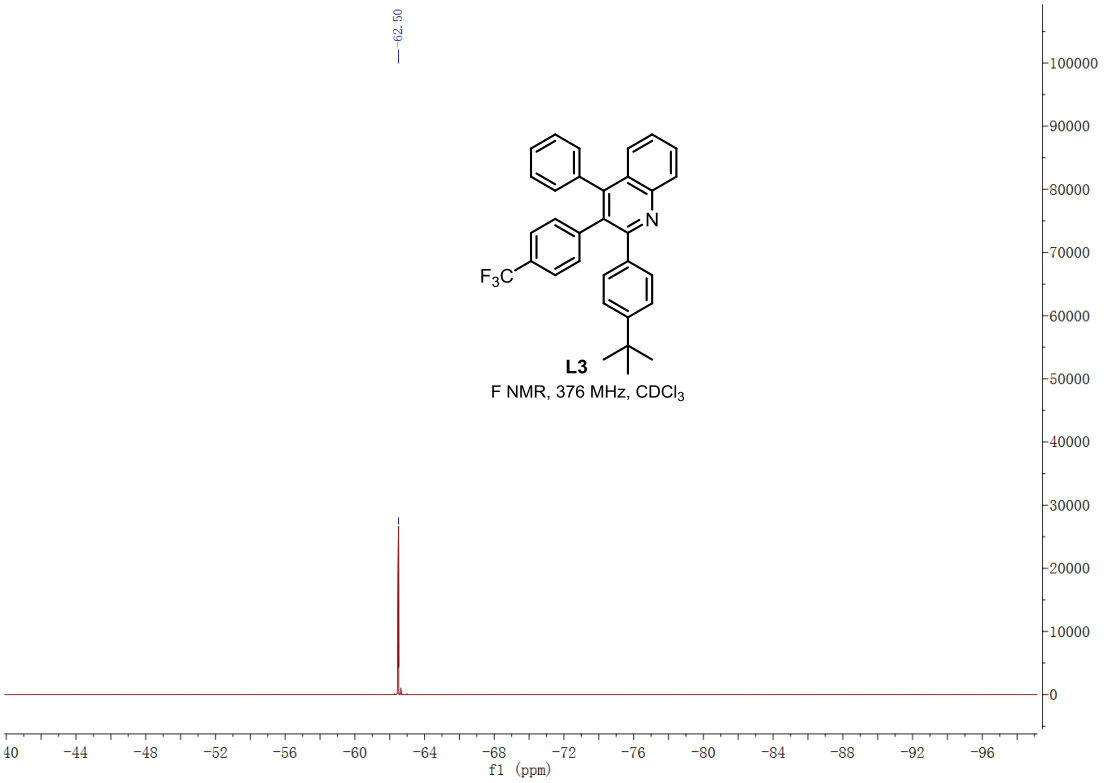

L3

F NMR, 376 MHz, $CDCl_3$

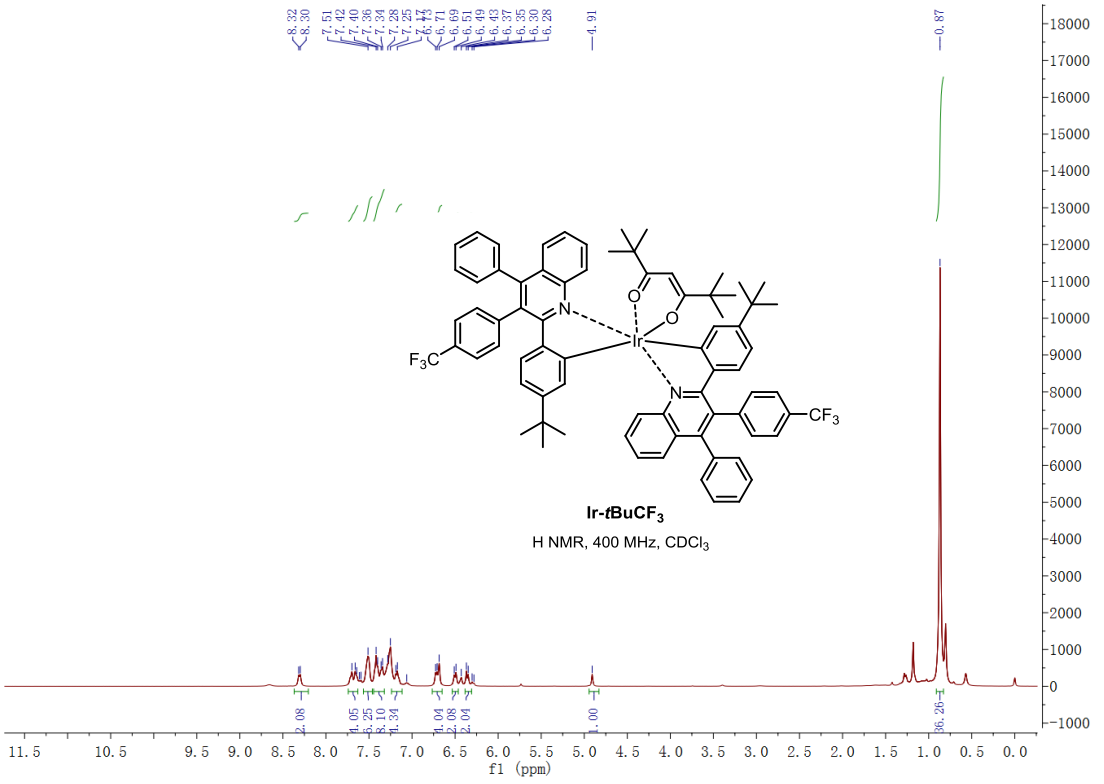

Ir-*t*BuCF$_3$

H NMR, 400 MHz, $CDCl_3$

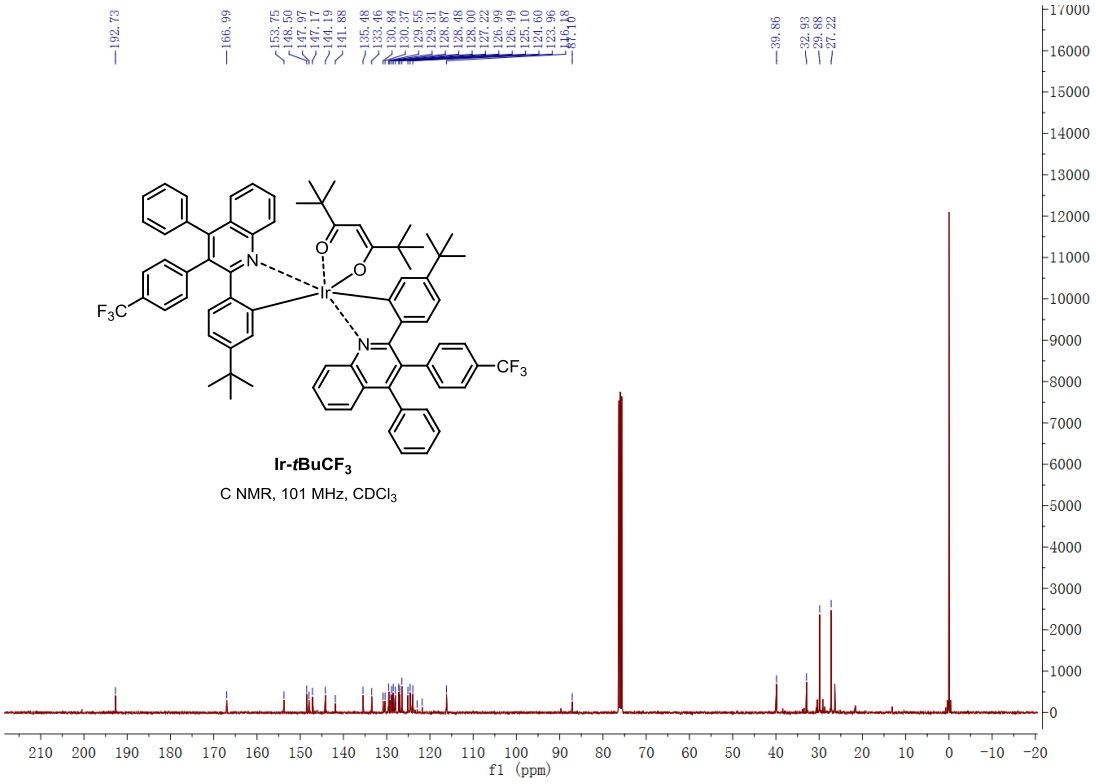

Ir-*t*BuCF$_3$

C NMR, 101 MHz, $CDCl_3$

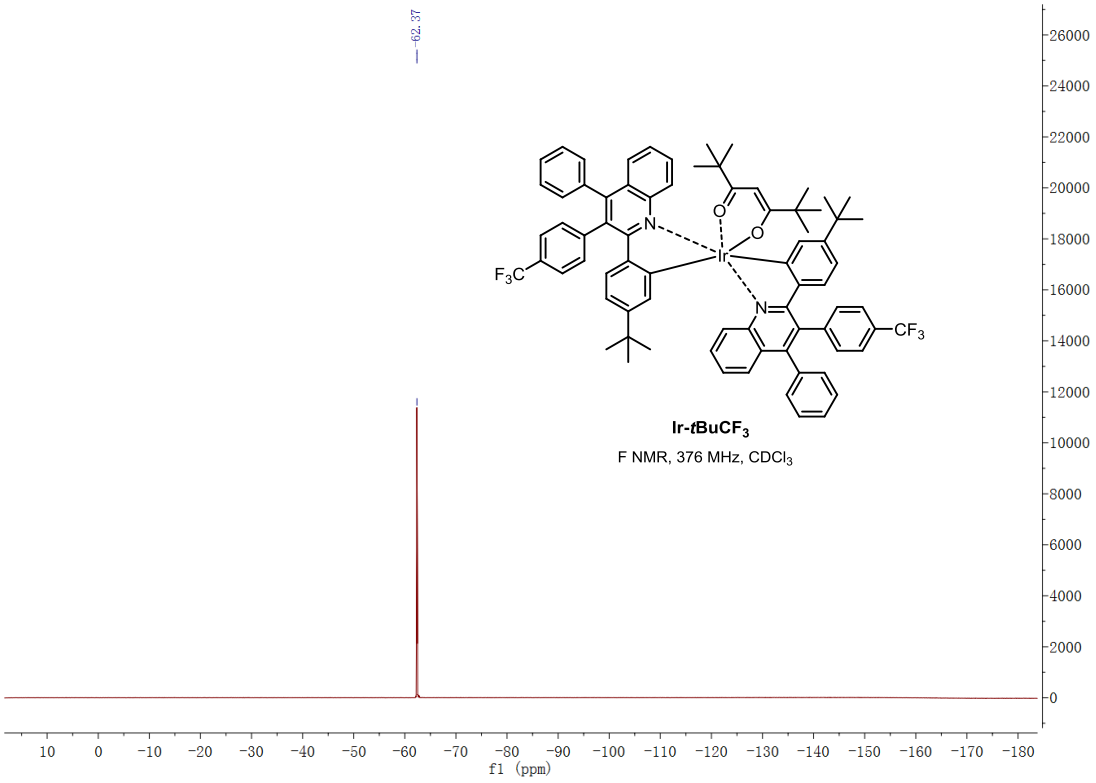

Ir-*t*BuCF$_3$

F NMR, 376 MHz, $CDCl_3$

2.4 HR Mass Spectra

Acquisition Parameter

Source Type	ESI	Ion Polarity	Positive	Set Nebulizer	0.4 Bar
Focus	Active	Set Capillary	4500 V	Set Dry Heater	180 °C
Scan Begin	50 m/z	Set End Plate Offset	-500 V	Set Dry Gas	4.0 l/min
Scan End	1500 m/z	Set Collision Cell RF	1040.0 Vpp	Set Divert Valve	Waste

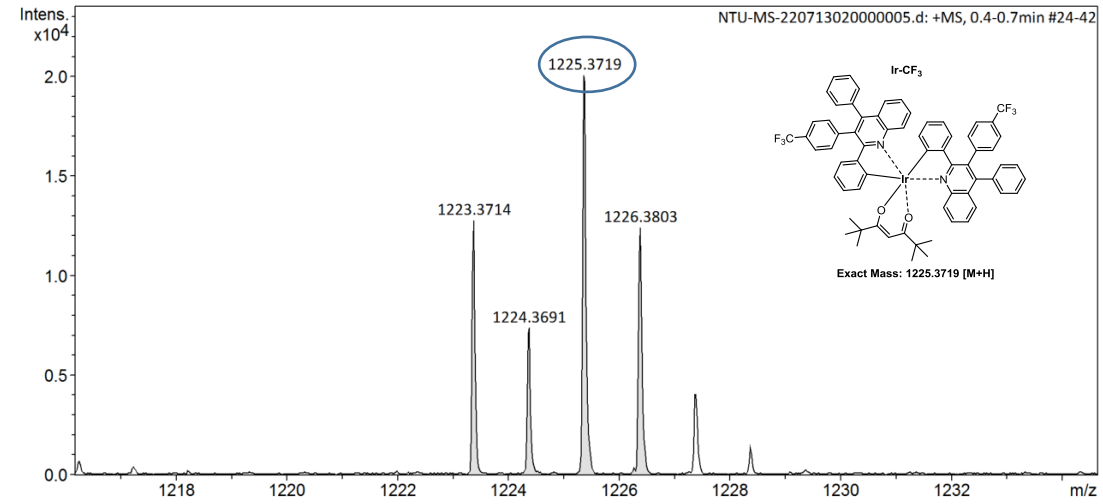

Acquisition Parameter

Source Type	ESI	Ion Polarity	Positive	Set Nebulizer	0.4 Bar
Focus	Active	Set Capillary	4500 V	Set Dry Heater	180 °C
Scan Begin	50 m/z	Set End Plate Offset	-500 V	Set Dry Gas	4.0 l/min
Scan End	1500 m/z	Set Collision Cell RF	1040.0 Vpp	Set Divert Valve	Waste

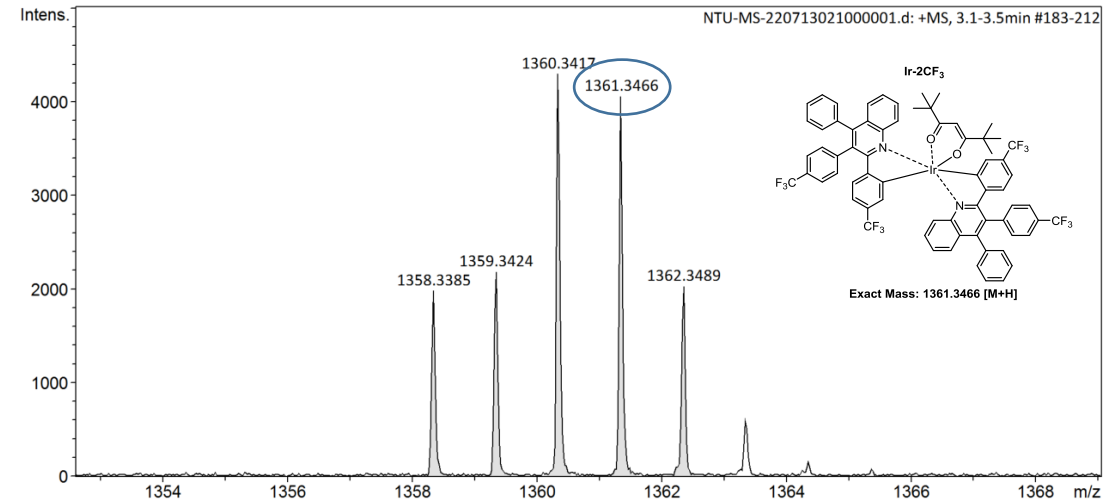

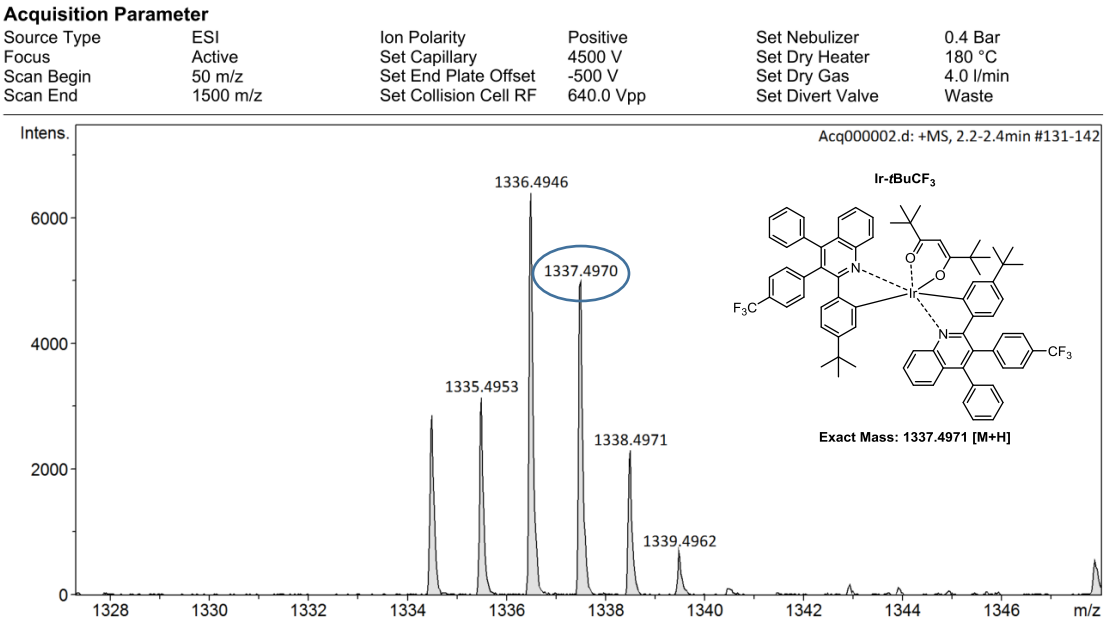

3. Supplementary data

Table S1 HOMO and LUMO electron cloud density distribution of each fragment of the Ir(III) complexes

Complex	Orbital	Energy/eV (Experiment)	Energy/eV (Calculated)	Composition (%)		
				Main Ligand	Ir	Ancillary Ligand
Ir-CF_3	HOMO	-5.19	-5.18	60.34	35.75	3.91
	LUMO	-2.89	-1.93	94.16	4.44	1.40
Ir-2CF_3	HOMO	-5.45	-5.51	42.14	36.11	21.75
	LUMO	-3.09	-2.22	94.06	4.42	1.52
Ir-*t*BuCF$_3$	HOMO	-5.11	-5.05	46.06	25.48	28.46
	LUMO	-2.85	-2.10	96.93	2.08	0.99

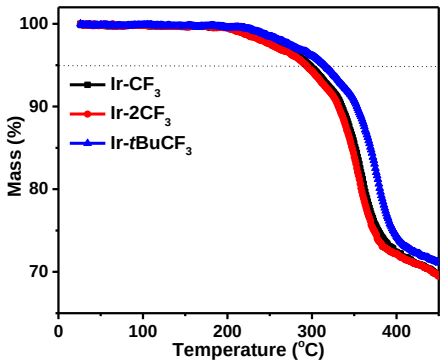

Fig. S1 Thermogravimetric analysis (TGA) of **Ir-CF$_3$**, **Ir-2CF$_3$** and **Ir-*t*BuCF$_3$**.

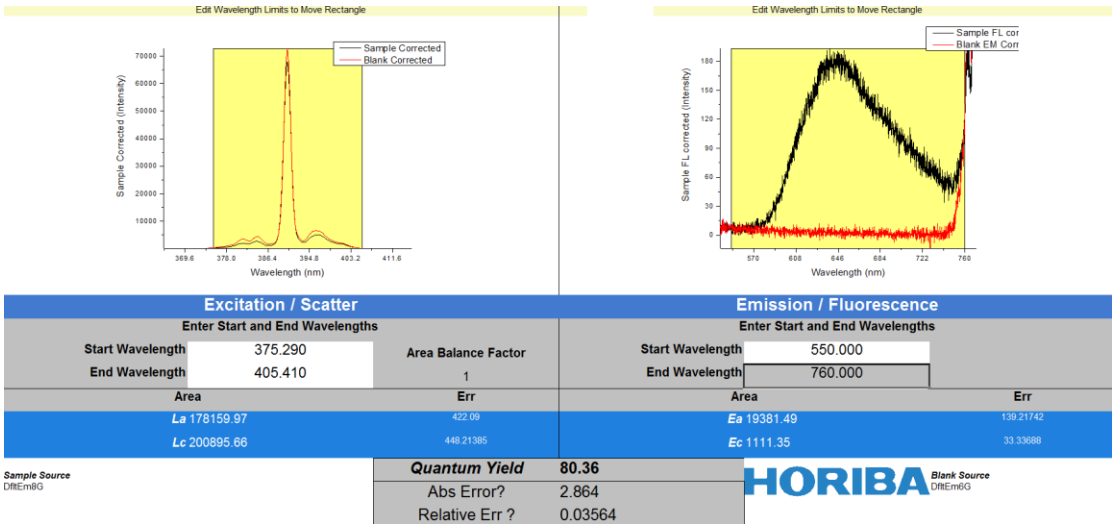

PLQY of **Ir-CF$_3$** in CH_2Cl_2

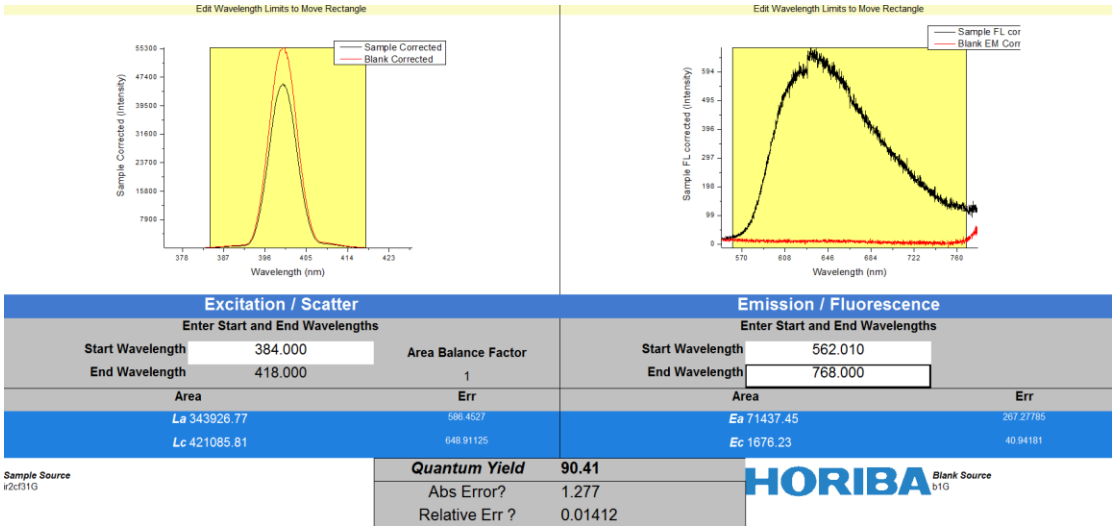

PLQY of **Ir-2CF$_3$** in CH_2Cl_2

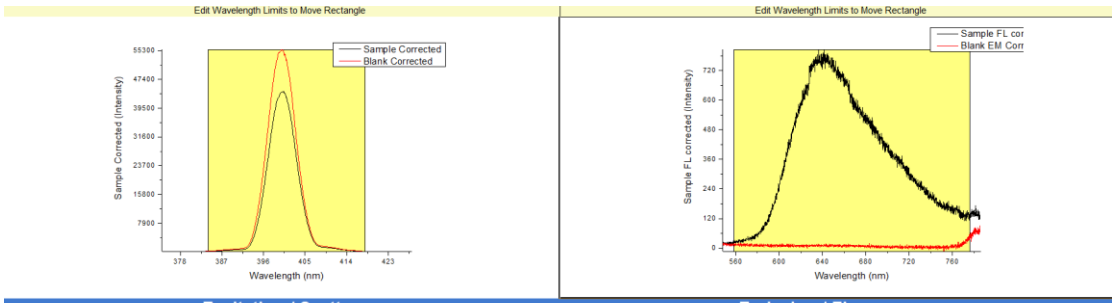

Excitation / Scatter			Emission / Fluorescence		
Enter Start and End Wavelengths			Enter Start and End Wavelengths		
Start Wavelength	384.000	Area Balance Factor	Start Wavelength	558.000	
End Wavelength	418.000	1	End Wavelength	776.000	
Area		Err	Area		Err
La	334113.88	578.02585	*Ea*	79850.63	282.57854
Lc	421085.81	648.91125	*Ec*	1947.68	44.13252

Quantum Yield	**89.57**
Abs Error?	1.116
Relative Err ?	0.01246

Sample Source tbuc1G — *Blank Source* b1G

PLQY of **Ir-*t*BuCF$_3$** in CH_2Cl_2

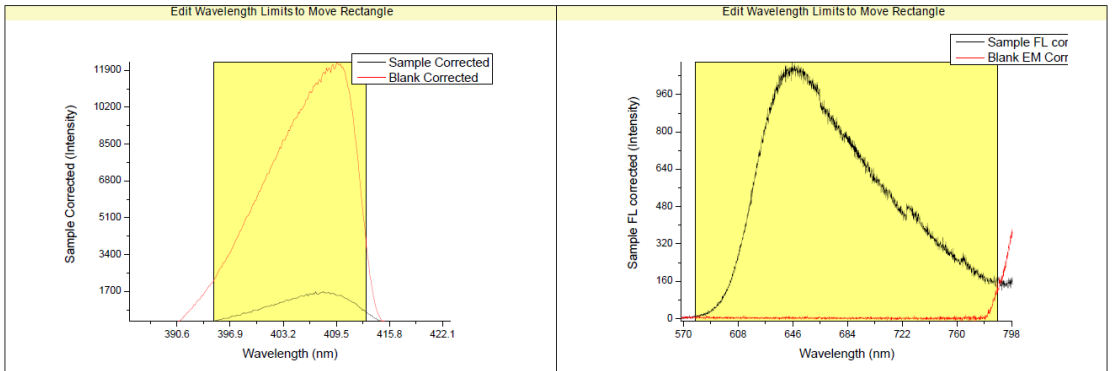

Excitation / Scatter			Emission / Fluorescence		
Enter Start and End Wavelengths			Enter Start and End Wavelengths		
Start Wavelength	395.000	Area Balance Factor	Start Wavelength	578.540	
End Wavelength	413.000	1	End Wavelength	788.570	
Area		Err	Area		Err
La	19806.46	140.73542	*Ea*	109556.49	330.99319
Lc	143805.62	379.21712	*Ec*	932.20	30.53199

Quantum Yield	**87.60**
Abs Error±	0.308
Relative Err ±	0.00352

Sample Source CF31G — *Blank Source* BLANK81G

PLQY of **Ir-CF$_3$** in doped film of 5 wt% in the 26DCzPPy

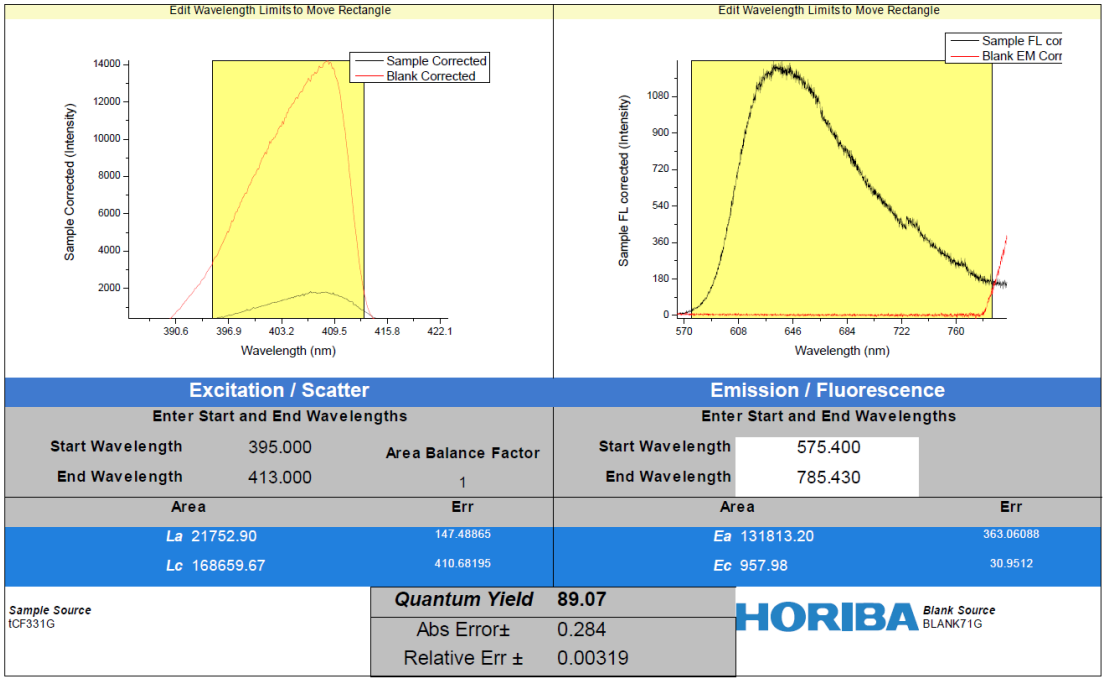

PLQY of **Ir-2CF$_3$** in doped film of 5 wt% in the 26DCzPPy

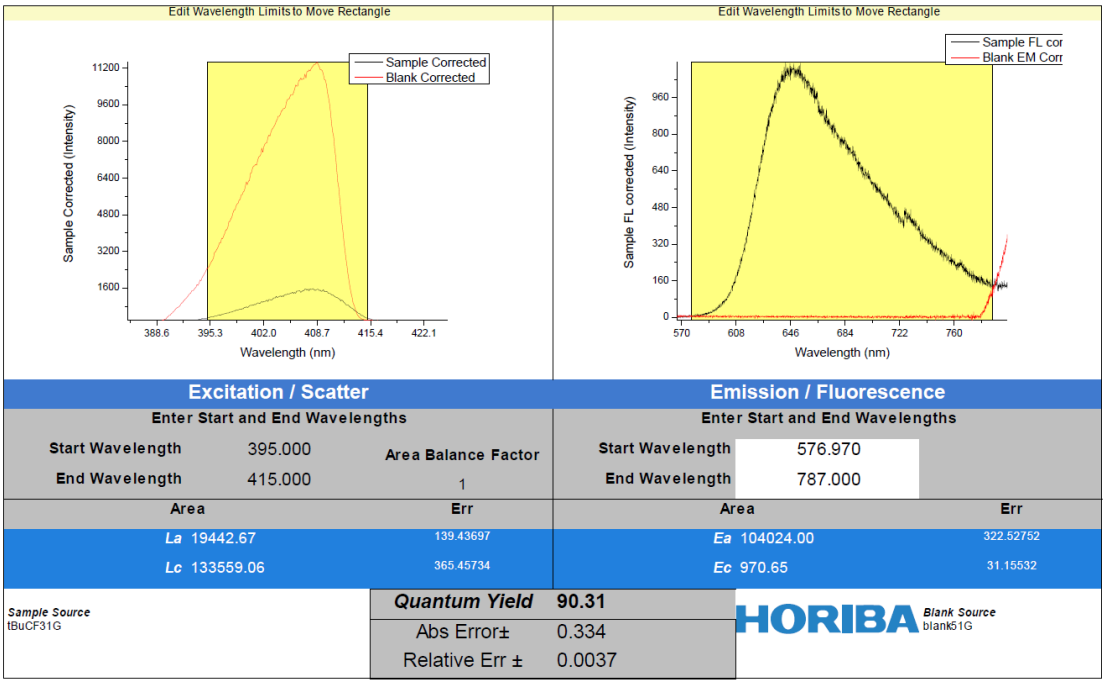

PLQY of **Ir-*t*BuCF$_3$** in doped film of 5 wt% in the 26DCzPPy

Fig. S2 The photoluminescence quantum yields (PLQYs) of **Ir-CF$_3$**, **Ir-2CF$_3$** and **Ir-*t*BuCF$_3$**.

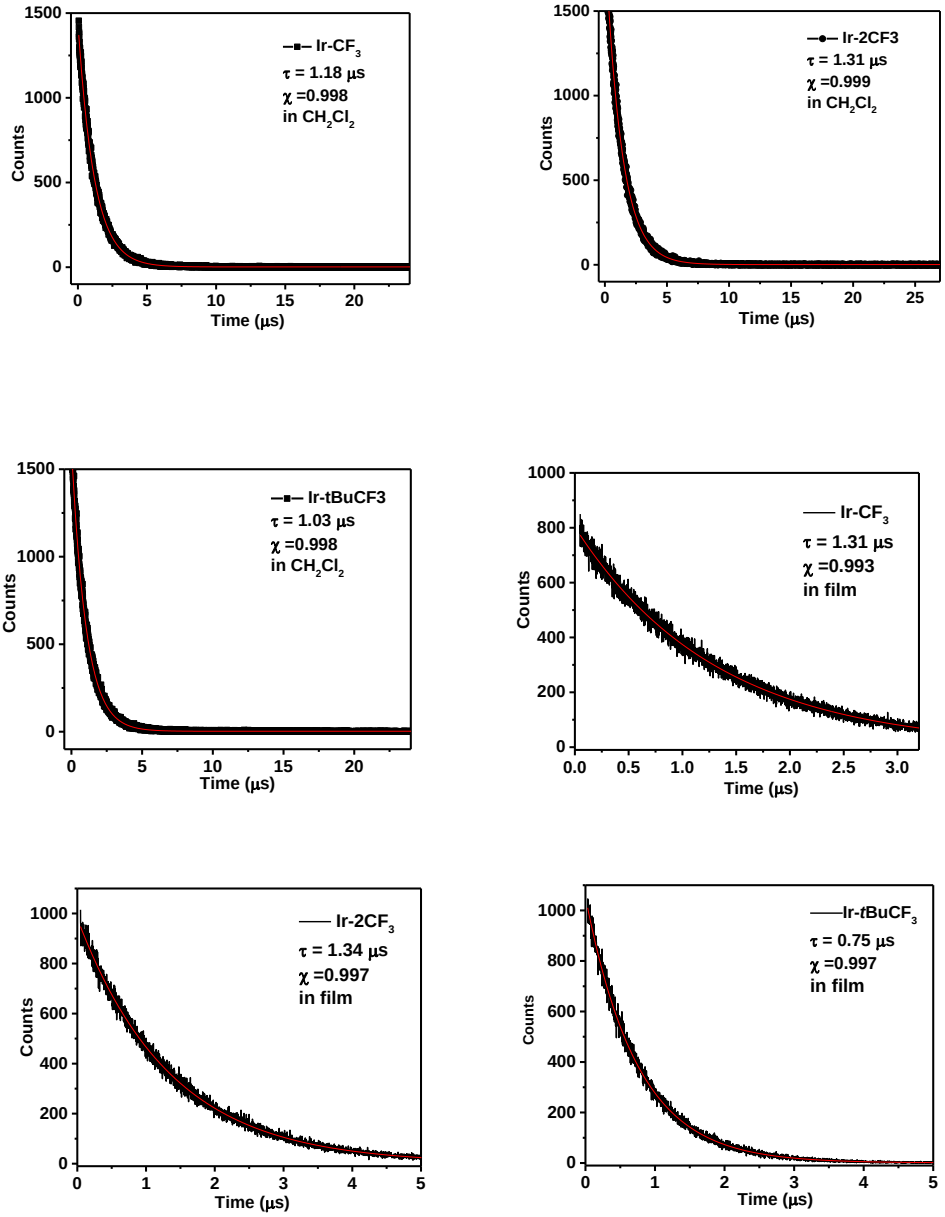

Fig. S3 The lifetime curves of **Ir-CF$_3$**, **Ir-2CF$_3$** and **Ir-*t*BuCF$_3$**.

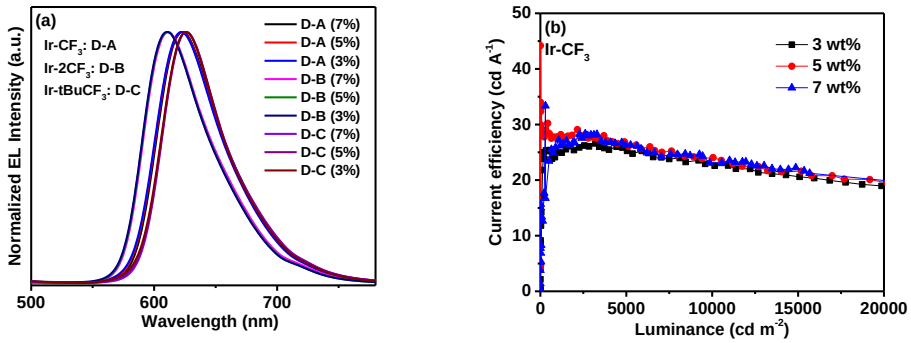

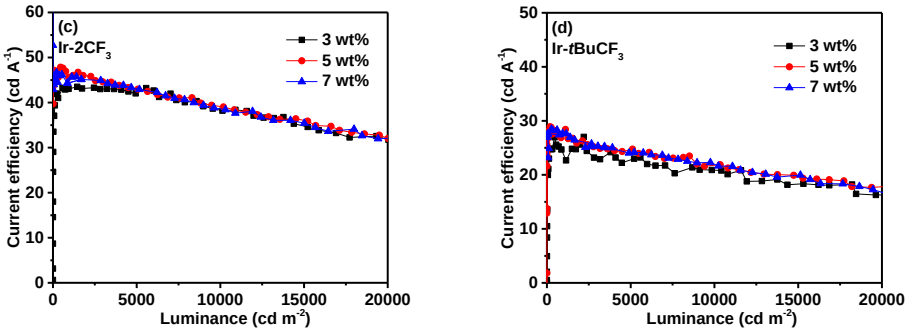

Fig. S4. EL performances in different doping concentrations: (a) EL spectra; (b), (c) and (d) current efficiency versus luminance curves.

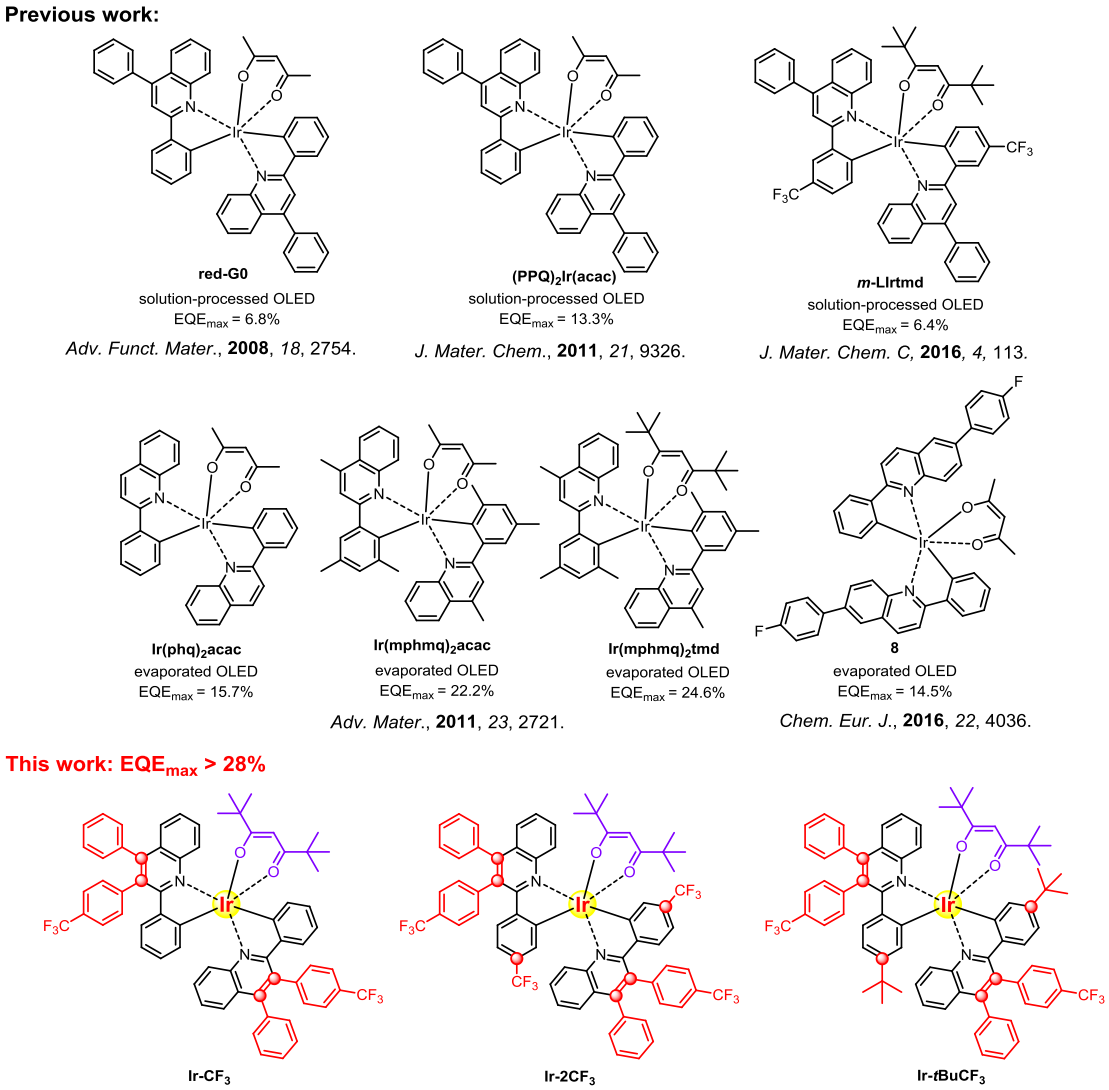

Fig. S5 The devices performances of 2-phenylquinoline ligand-based Ir(III) complexes.